Oxidation of photochromic spirooxazines by coinage metal cations. Part I. Reaction with $AgNO_3$: formation and characterisation of silver particles

Pawel Uznanski,*[a] Catherine Amiens,[b] Bruno Donnadieu,[b] Yannick Coppel[b] and Bruno Chaudret[b]

[a] *Centre for Molecular and Macromolecular Studies, Polish Academy of Sciences, Sienkiewicza 112, 90-363 Lodz, Poland. E-mail: puznansk@bilbo.cbmm.lodz.pl*

[b] *Laboratoire de Chimie de Coordination, CNRS, 205 Route de Narbonne, F-31077 Toulouse cedex 4, France. E-mail: chaudret@lcc-toulouse.fr, amiens@lcc-toulouse.fr*

Received (in Montpellier, France) 18th June 2001, Accepted 12th September 2001
First published as an Advance Article on the web

Thermal oxidation of the zwitterionic form of two photochromic spirooxazines: 1,3-dihydro-1,3,3-trimethylspiro(2*H*-indole-2,3′-[3*H*]naphth[2,1-*b*]-[1,4]oxazine) (**1**) and 1,3-dihydro-1,3,3-trimethylspiro(2*H*-indole-2,3′-[3*H*]phenanthr[9,10-*b*]-[1,4]oxazine) (**2**) has been studied in the presence of silver ions in anaerobic conditions. The products of the reaction have been identified and a mechanism for their formation is proposed. In alcohols (MeOH, EtOH), the major degradation product is the indolinooxazole salt together with either methoxy- or ethoxy-substituted spirooxazines at the C2′ carbon atom of the C2′=N1′ bond. The four new spirooxazine derivatives display no photochromic properties although X-ray diffraction studies show that the bond lengths around the spiro carbon atom are similar to those observed for compounds revealing colouration. Photophysical properties of the indolinooxazole and of its hydroxylated derivative are also presented. High quantum yield and large Stokes shifts are observed. As a consequence of the reduction of silver ions to neutral atoms, silver colloids have been prepared after either thermal- or photo-oxidation of spirooxazine. They are stabilised by poly(*N*-vinylpyrrolidone). The formation and growth of silver colloids have been studied by electron microscopy, photon correlation spectroscopy and UV-vis absorption spectroscopy. The growth of silver particles of different sizes and morphologies is presented and the role of a photochromic electron donor on the growth process is discussed. The average particle sizes ranged from a few to approximately one hundred nanometers. The classical plasmon absorption band at 420 nm and a broad red-shifted peak at 790 nm due to the large non-spherical particles are thus observed. Both particle size and plasmon absorption are dependent upon UV irradiation. Size enlargement upon irradiation of silver colloids brings about colour changes from yellow through green to light blue.

Spirooxazines (SO), which are photochromic, reveal many interesting properties, with regard to their photocolouration[1] and photodegradation[2–4], compared to the closely related and more intensively studied spiropyrans. The photochromic properties of these compounds are due to C–O bond cleavage induced by UV irradiation or heating, followed by the formation of coloured, metastable merocyanine (Mc) entities (Scheme 1). The replacement of the pyran ring by an oxazine ring generally improves the resistance of the compound to prolonged UV irradiation. A good understanding of

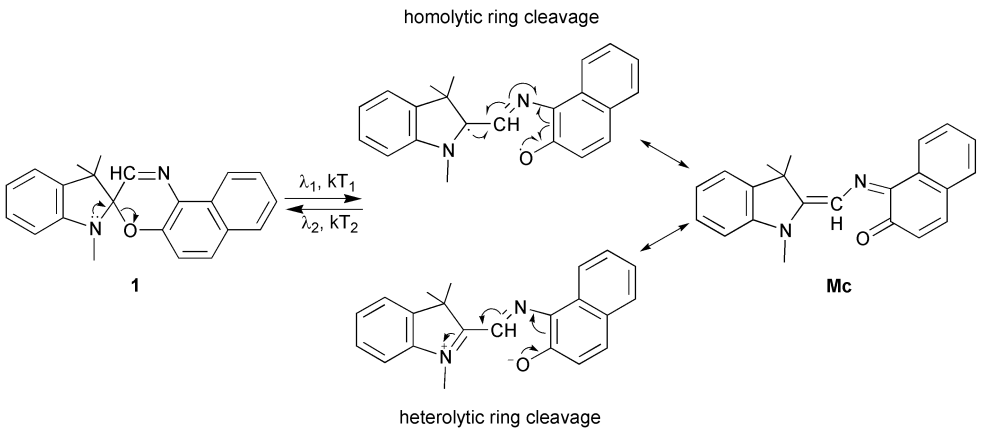

Scheme 1

 DOI: 10.1039/b105446p

fundamental phenomena which accompany the ring-opening reaction is important if spirooxazines are to be used as functional dyes[5] or for commercial applications. Recent research on photochromism has been focused on the elucidation of photochemical and photophysical mechanisms using Raman spectroscopy.[6,7] In particular, surface-enhanced spectroscopies including surface-enhanced Raman spectroscopy have become important in fundamental physical and chemical research.[8,9] Silver colloids are used as enhancement-active substrates for structural identification of traces of photochromes adsorbed on metallic surfaces and detection of their photodegradation products under photolysing laser light. Surface-sensitive phenomena are also observed in nanostructured assemblies consisting of metallic colloidal particles and photoactive dyes. In this case colloidal particles significantly enhance the photoactivity of such systems. In an attempt to study the adsorption of spirooxazines on Ag particles we have observed that, if the colloidal solution contained Ag^+ ions, spirooxazines underwent fast thermal degradation together with formation of a thin mirror layer, or colloidal solution in the presence of a stabilising agent. This finding could be important not only in relation to spiro compounds but to some other organic dyes as silver salts are often used as precursors for sol preparation. This prompted us to study the reactivity of spirooxazines with silver salts.

In this paper we report a study of the mechanism of thermal oxidation reactions of spironaphthoxazine (**1**) and spirophenanthroxazine (**2**) by silver nitrate in polar solvents (CH_3OH, C_2H_5OH, and CH_3CN) and the identification of products involved in the degradation process. Silver nanoparticles and nanocrystallites formed after metal reduction were characterised in the presence of the stabilising agent poly(*N*-vinylpyrrolidone) (PVP).

Results and discussion

Photoirradiation

In ethanol solution, the thermal equilibrium between the parent form **1** and its merocyanine isomer is strongly shifted towards the closed form and the solution is colourless (Scheme 1). Under UV irradiation the optical absorption spectrum shows a new band, connected with the open Mc form, with a maximum at 610 nm and a shoulder at 578 nm. The presence of silver nitrate caused extensive colouration under short photoirradiation times (< 10 s) with a prominent new peak at 522 nm [Fig. 1(a)]. The photocolouration of the freshly prepared solution is thermally reversible with a first order kinetic constant $k = 0.03\ s^{-1}$, much slower than the thermal decay rate measured for a neat photochrome solution ($k = 0.212\ s^{-1}$). The hypsochromic shift of the absorption maximum and the slowing down of the thermal decolouration implies that the coloured open Mc form is stabilised, probably through an interaction between the carbonyl oxygen atom and a silver ion, thus suggesting that the ring opening follows a heterolytic pathway (Scheme 1). This co-ordination is similar to that observed for a spirooxazine derivative containing a crown moiety in the presence of lithium ions[10] or for spiroquinoxazine and bivalent metal ions,[11] which become effective chelators after thermally or photochemically induced ring opening. Furthermore, it is well known that under acidic conditions the spiro form can be phototransformed into a protonated open form with a characteristic blue-shifted visible absorption band ($\lambda_{max} = 520$ nm).[12]

Upon prolonged irradiation, in photostationary conditions, the intensity of the band at 522 nm gradually decreases while a new one at 448 nm emerges along with a broad background in the red region [Fig. 1(b)]. During these transformations four isosbestic points at 296, 370, 492 and 590 nm are observed. The process is now thermally irreversible. At the end of the process, the solution is orange and strongly fluorescent with yellow transparent sediment on the walls of the reaction flask [Fig. 1(b), curve E]. The spectrum has a maximum at 430 nm, which is related to the plasmon band of the formed nanosized silver particles. This absorption band results from interactions of free electrons confined to small metallic spherical objects with incident electromagnetic radiation. Colloidal silver is transparent in the visible and IR region, unlike bulk silver, which absorbs strongly.

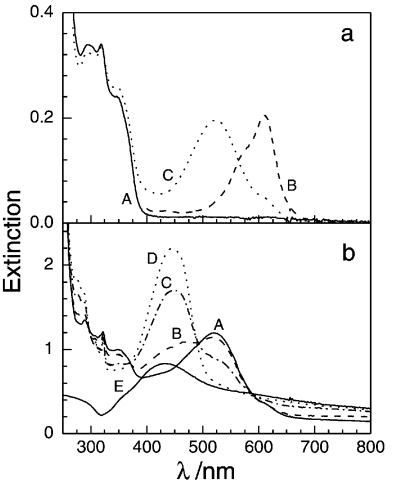

Fig. 1 (a) The absorption spectrum of a freshly prepared solution of **1** (5×10^{-3} M) in ethanol (A), after 10 s illumination with 320–360 nm light from an 8 W luminescence lamp (B), and a similarly irradiated solution also containing 10^{-2} M $AgNO_3$ (C). (b) Absorption spectral changes of **1** and $AgNO_3$ (1 : 2) in ethanol produced by prolonged UV illumination for 10, 15, 25 and 35 min. (curves A–D, respectively). Spectrum E is a plasmon band of silver particles sedimented on the cuvette windows.

Thermal oxidative dark reaction

The spectral changes recorded during the dark reaction of **1** in the presence of silver nitrate (1 : 2 stoichiometric ratio) in dry MeOH are similar to those recorded for samples exposed to prolonged UV irradiation. In particular, a band attributed to an interaction with silver ions was observed, suggesting that the ring-opening process follows a heterolytic route. The thermal reaction is slow at room temperature (20 °C) and takes several hours to be completed. This suggests that that the ring opening is the rate-determining step. The influence of silver nitrate on the ^1H NMR spectrum of **1** confirms the formation of an open Mc form in the first stage of reaction. The resonance of the proton on C2′ shifts downfield from 7.82 to 10.17 ppm and finally disappears from the spectrum. Similarly the singlet located at 2.75 ppm, attributed to the methyl on the N atom of the indoline moiety, shifts downfield to 3.63 ppm and finally to 4.82 ppm.

Malatesta *et al.*[4] demonstrated that photochromic spirooxazines readily undergo oxidative degradation in the presence of an electron acceptor and in oxygen-free solution. They reported that in the dark the oxidative degradation proceeds through an electron transfer process from the spirooxazine to the appropriate electron acceptor molecule. The final product is a salt of an indolinonaphthoxazole derivative, which can be considered as a product of rearrangement. In our case the thermal reaction of **1** with silver nitrate in methanol yields two major products: a nitrate salt **3** and a new compound **4** (Scheme 2), as deduced from ^1H NMR spectra in MeOH-d_4 and an X-ray diffraction study. Analytically pure samples of **4** were isolated as single crystals (20% yield) from the concentrated reaction solution at low temperature. In the presence

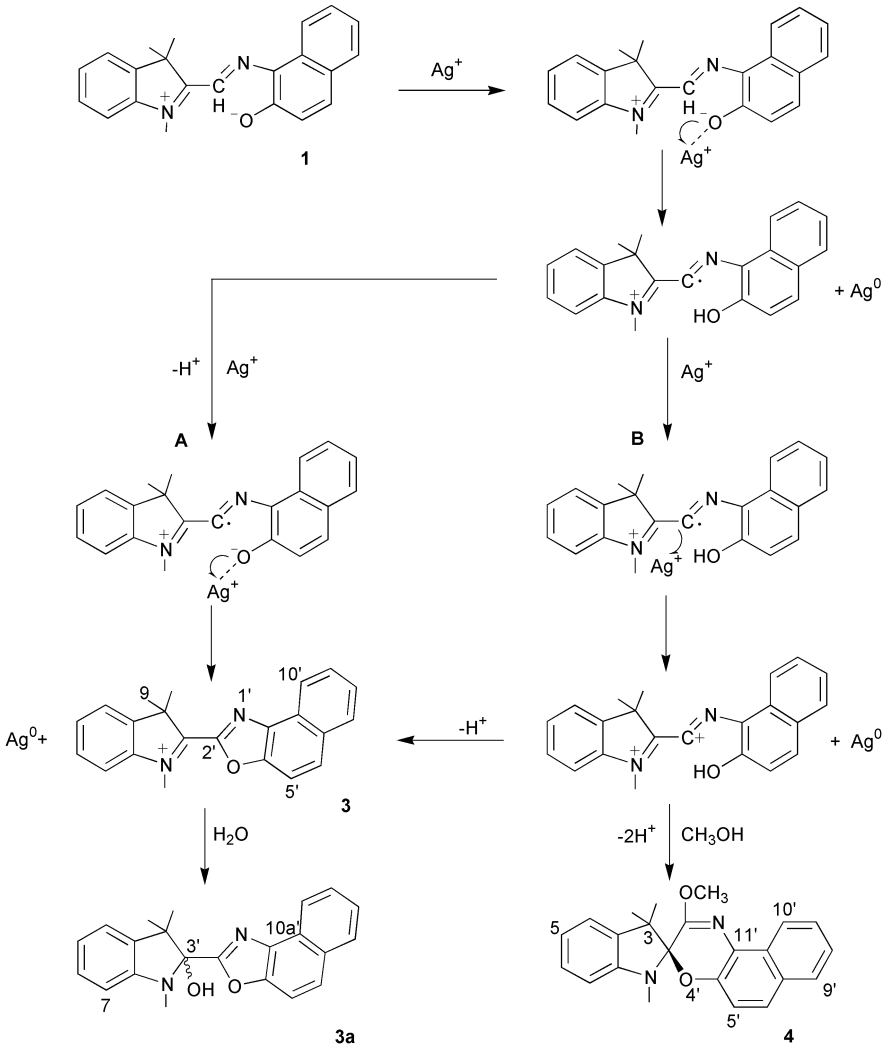

Scheme 2

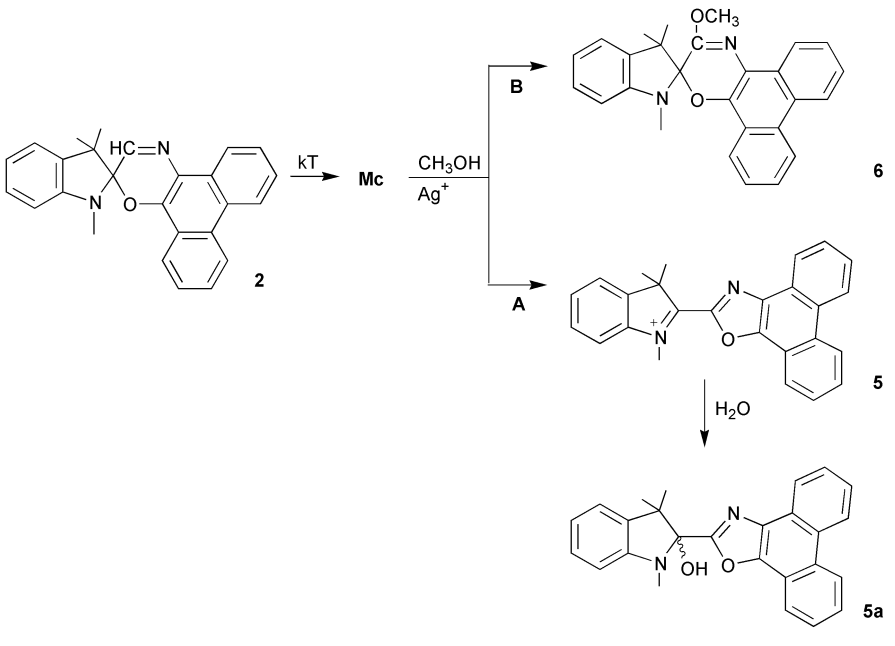

Scheme 3

of water, **3** is converted to (hydroxyindolino)naphthoxazole **3a**. In refluxing acetonitrile the reaction of **1** and $AgNO_3$ provides only the salt **3**, which precipitates from solution as an orange–brown powder. Unfortunately, attempts to crystallise the product failed, in contrast to derivatives of **1** substituted in the 4 or/and 5 positions on the indoline part, which were reported to crystallise easily.[4]

First of all, it is important to note that all experiments were carried out under an inert atmosphere of argon, thus ruling out the possible formation of **3** from a radical oxidation *via* a transient complex [$Mc^{\bullet+}/O_2^{\bullet-}$] as observed by Malatesta *et al.*[3,4] In order to explain the formation of **3** and **4** we propose that the thermal oxidation proceeds according to two complementary pathways (A and B, Scheme 2). They involve two electron transfers from the O4′ oxygen atom or C2′ carbon atom to a silver cation. After heterolytic opening of the spirooxazine and co-ordination of the silver ion to the Mc form, a first electron transfer occurs leading to the formation of a radical species at oxygen. Fast 1,5-hydrogen transfer forms a more stable carbon radical. This radical can subsequently undergo two different reactions. Path A (radical route) supposes a deprotonation step of the hydroxyl group, activated by Ag^+ acting as a Lewis acid, followed by a further electron transfer to another silver ion. This leads directly to **3**, through an intramolecular radical recombination. Path B (polar route) supposes a direct electron transfer from the radical at carbon C2 to the silver ion. The dicationic species thus formed should be highly sensitive to nucleophilic attack. An alkoxy group could then be easily incorporated in the structure, when reacting in alcohol. This charge-separated transient species may also be rearranged directly into **3**. It should noted that in acetonitrile, only **3** is observed.

It is noteworthy that alcohol is not able to reduce Ag^+ ions at room temperature. Thus, the pathway involving hydrogen atom abstraction from MeOH and attack of the methoxyl radical $CH_3O^{\bullet}$ on the C2′ position is hardly probable.

When the phenanthrene analogue **2** was used in the reaction with $AgNO_3$ in methanol, a salt **5** and a methoxy derivative **6** were obtained (Scheme 3). Similarly to product **3**, **5** is not stable and slowly converts to the neutral species **5a** (both MeOH and $AgNO_3$ could contain traces of water).

In refluxing ethanol, oxidative reaction of **1** afforded the spiro product **7**, which separated as single crystals during the slow evaporation of the solvent at room temperature (Scheme 4). The structure of **7** with a nitro group at the C5 carbon suggests that, at high temperature, nitration takes place as a result of the presence of nitric acid in the mixture.

X-Ray crystallographic results

The solid state structures of **4**, **4**-d_3, **6** and **7** are similar to those of other photochromic spirooxazines and spiropyrans.[13] The compounds consist of an indoline part orthogonally linked through the spiro carbon to the oxazine ring with a methoxy or ethoxy substituent at the C atom adjacent to the oxazine nitrogen. Selected bond lengths and angles around the spiro carbon atom are given, together with their molecular structures, in Fig. 2–4. The effect of the substitution on the oxazine ring is unambiguous: for **4** and **4**-d_3 the indoline moieties are bent towards O1 whereas for **6** and **7** the spiro carbon atom

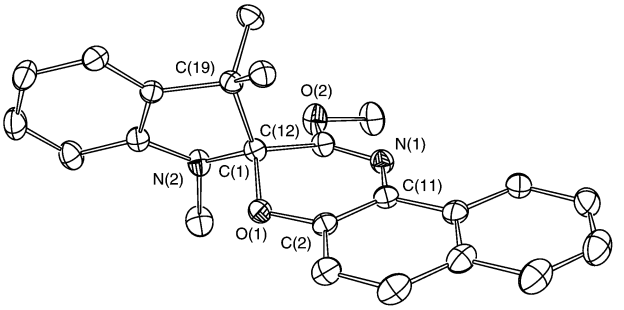

Fig. 2 The structure of **4** with thermal ellipsoids at the 40% level. Selected bond lengths (Å) and angles (°) around the spiro carbon atom are as follows: O(1)–C(1), 1.4595(16); O(1)–C(2), 1.3674(17); N(2)–C(1), 1.4275(17); C(1)–C(12), 1.5182(19); C(1)–C(19), 1.570(2); C(12)–N(1), 1.267(2); N(2)–C(1)–O(1), 106.62(10); N(2)–C(1)–C(12), 113.61(11); O(1)–C(1)–C(12), 107.16(12); N(2)–C(1)–C(19), 103.52(12); O(1)–C(1)–C(19), 110.13(10); C(12)–C(1)–C(19), 115.48(11).

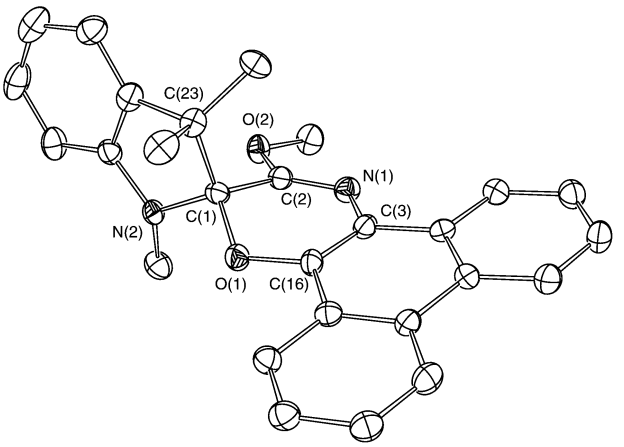

Fig. 3 The structure of **6** with thermal ellipsoids at the 40% level. Selected bond lengths (Å) and angles (°) around the spiro carbon atom are as follows: N(2)–C(1), 1.427(6); O(1)–C(1), 1.441(5); C(1)–C(2), 1.510(6); C(1)–C(23), 1.582(6); C(2)–N(1), 1.280(5); O(1)–C(16), 1.384(5); N(2)–C(1)–O(1), 106.2(3); N(2)–C(1)–C(2), 113.8(4); O(1)–C(1)–C(2), 106.8(3); N(2)–C(1)–C(23), 103.9(3); O(1)–C(1)–C(23), 113.2(3); C(2)–C(1)–C(23), 113.0(4).

distorts the indoline plane towards C2. In all compounds the oxazine ring is folded towards the *gem*-methyl groups. The structures exist only in closed form and do not exhibit any photochromic behaviour. The C_{spiro}–O distances directly responsible for the photochromic properties are similar in the four spirooxazine products with values comparable to compounds revealing photoreactivity. Previous reports suggest that the presence of an additional bulky substituent on the oxazine part interferes with ring opening during the photochromic reaction and that steric effects account for the non-photochromic properties.[14] However, when the indoline and naphthoxazine moieties are linked by an alkyl chain the configuration can be considered as rigid but cleavage still occurs in a polar solvent.[15] Thus, it can not be excluded that electronic effects inducing changes in the C–O bond polarization due to

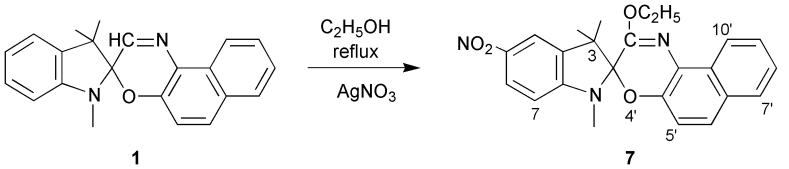

1 **7**

Scheme 4

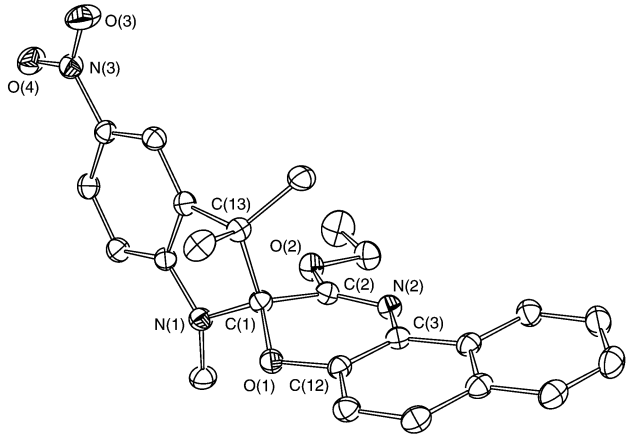

Fig. 4 The structure of **7** with thermal ellipsoids at the 40% probability level. Selected bond lengths (Å) and angles (°) around the spiro carbon atom are as follows: O(1)–C(12), 1.3784(2); O(1)–C(1), 1.4303(2); N(1)–C(1), 1.4463(2); N(2)–C(2), 1.2671(2); C(1)–C(2), 1.5243(2); C(1)–C(13), 1.573(2); O(1)–C(1)–N(1), 106.29(1); O(1)–C(1)–C(2), 107.76(1); N(1)–C(1)–C(2), 112.23(1); O(1)–C(1)–C(13), 114.12(1); N(1)–C(1)–C(13), 104.18(1); C(2)–C(1)–C(13), 112.16(1).

electron-donating substitution on C2′ may be responsible for the loss of photochromic activity. Interestingly, a derivative with a deuterated methoxy substituent, which was introduced during the reaction in methanol-d_4, displays different crystal packing than compound **4** (Table 1).

Photophysical properties of 3 and 3a

The oxidation products **3** and **3a** of spirooxazine strongly emit bluish and greenish fluorescence, respectively. Thus fluorescence is indicative of electron transfer processes from the photochromic dye to the electron acceptor. Within this context photophysical studies of the final products were undertaken.

The absorption spectrum of the indolinooxazole salt **3** in acetonitrile displays one broad and intense peak at 466 nm ($\varepsilon = 6.35 \times 10^4$ M^{-1} cm^{-1}), while the spectrum of the (hydroxyindolino)oxazole derivative **3a** is blue shifted ($\lambda_{max} = 371$ nm, $\varepsilon = 1.63 \times 10^4$ M^{-1} cm^{-1}), more structured and less intense. In contrast to the parent spirooxazine **1**, **3** and **3a** exhibit a strong fluorescence, respectively orange ($\lambda_{max} = 535$ nm) and blue ($\lambda_{max} = 448$ nm). The excitation spectra match the absorption ones for both compounds, showing that internal conversion from the upper excited singlet states to the lowest one proceeds with unit quantum efficiency.

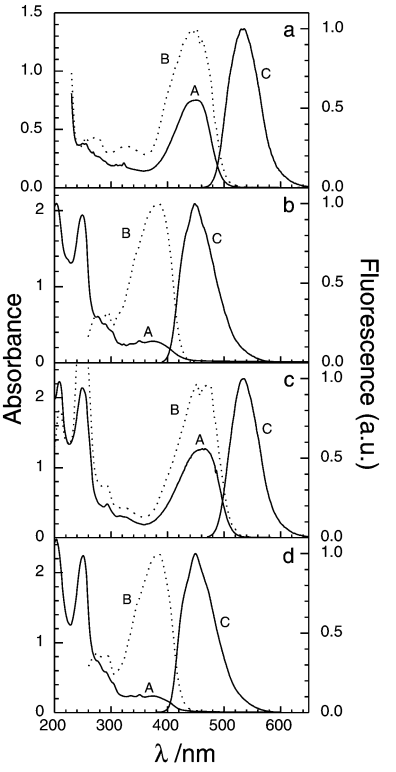

Fig. 5 UV-vis absorption (A), fluorescence excitation (B) and emission (C) spectra. (a) **3** in acetonitrile; (b) **3a** in EtOH; (c) **5** in acetonitrile; (d) **5a** in EtOH.

The Stokes shift is quite large: 3500 cm^{-1} for **3** and 4000 cm^{-1} for **3a**, indicating that the ground and fluorescence states have different geometries. The fluorescence lifetime can be fitted with a single exponential yielding lifetimes of 4.1 and 2.9 ns; the fluorescence quantum yield φ_f is 0.83 and 0.23 for **3** and **3a**, respectively. The calculated radiative lifetimes τ_{rad} ($= \tau_f/\varphi_f$) of the emitting states are respectively 5 and 12.6 ns. The photophysical properties of **5** and **5a** are very similar to those of **3** and **3a** (Fig. 5), showing that these properties are not much affected by substitution on the oxazoline part.

Electronic absorption spectra of the spirooxazine derivatives 4, 6 and 7

These products are non-photochromic and resistant to oxidation processes. The ultraviolet spectra of **4**, **6** and **7** (Fig. 6)

Table 1 Crystallographic data for spirooxazine compounds

	4	**4**-d_3	**6**	**7**
Formula	$C_{23}H_{22}N_2O_2$	$C_{23}H_{22}N_2O_2$	$C_{27}H_{24}N_2O_2$	$C_{24}H_{23}N_3O_4$
FW	358.43	358.43	408.48	417.45
Space group	$P2_1/c$	$C2/c$	$P2_1/c$	$P2_1/c$
Crystal system	Monoclinic	Monoclinic	Monoclinic	Monoclinic
a/Å	16.6277(2)	27.659(3)	13.450(3)	10.3622(9)
b/Å	8.2069(7)	8.4635(1)	20.456(4)	15.3310(2)
c/Å	15.1464(2)	16.5591(2)	7.667(2)	13.5407(1)
β/°	116.113(1)	100.371(1)	96.61(3)	103.856(1)
U/Å^3	1855.9(3)	3813.1(7)	2095.4(8)	2088.5(3)
Z	4	8	4	4
T/K	180	298	180	180
Reflections collected	13104	13382	12417	16036
Unique reflections	3449	2744	2978	3872
R_{int}	0.0360	0.0801	0.1076	0.0371
R	0.0403	0.0471	0.0603	0.0399
wR	0.0932	0.1157	0.1441	0.1011

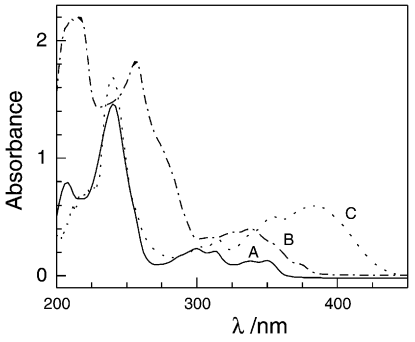

Fig. 6 UV-vis absorption spectra in chloroform: **4** (A), **6** (B), **7** (C).

show two structured bands of medium intensity in the region 280–440 nm and two peaks in the region 200–280 nm with an intensity approximately six times greater then that of their parent forms **1** or **2**. The positions of the bands, in the long-wavelength region, are little affected by the presence of the methoxy substituents but simultaneously are better resolved. In contrast, the presence of a nitro group on the indoline moiety both increases the intensity of the most intense band and shifts it by 35 nm to the red, leaving the band at 314 nm unaffected.

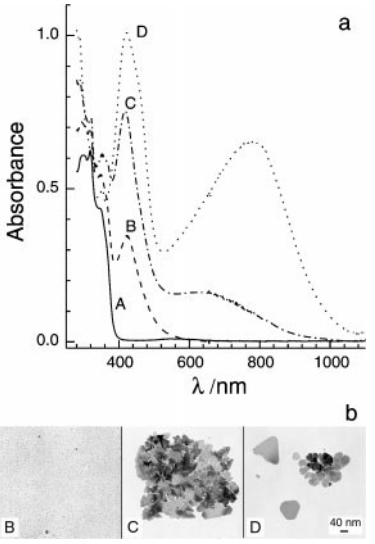

Fig. 7 Extinction spectra of silver colloid produced during thermal reduction of silver nitrate by **1** in the presence of PVP in ethanol at room temperature. (a) Spectrum of a freshly prepared solution (A), after 2 h (B), after 7 h (C), after 20 h (D). The shoulder at 460 nm in spectrum D is due to the absorption of **2**. (b) TEM micrographs of samples corresponding to the successive stages of colloid formation.

Optical properties of the silver colloids

When the thermal oxidation of **1** with $AgNO_3$ in an alcoholic solution is carried out in the presence of PVP, colloidal silver is produced. The formation of nanometre size metal clusters can be easily followed by UV-vis absorption spectroscopy since the sol displays the classical plasmon absorption band of silver resulting from the coupling of the surface plasma oscillation modes of conduction electrons with incident electromagnetic field.[16] Two maxima in the absorption spectrum are observed [Fig. 7(a)]. At the beginning of the reaction a peak in the blue region around 420 nm is formed, which is due to absorption by silver spheres below 20 nm in diameter. During the course of the reaction, a new broad band in the long-wavelength region emerges and gradually shifts toward longer wavelengths with a simultaneous increase in its intensity. The colour of the colloidal sample thus changes from yellow through light green and finally turns to dark green. At the end the colloidal samples were found to be stable, keeping their colour for months.

Electronic modes in silver particles are particularly sensitive to their shape and size, leading to pronounced effects in the visible part of the spectrum. Theoretical studies show that the absorption spectrum splits, as the size of particles becomes larger.[17] Our Transmission electron microscopy (TEM) results are in agreement with these studies [Fig. 7(b)]. Various silver aggregates were identified during the different stages of the reaction. At the beginning, spherical particles with diameters of a few nanometers to 20 nm are formed, then lumps of about 100 nm (composed of rather large sintered particles) and finally large individual non-spherical objects and particles with well-defined edges (either triangles or triangles with cut tops). Similar observations were reported for radiolytically induced reduction of silver ions in the presence of organic ligands.[18] The uniform contrast of these particles observed under TEM suggests that the thickness of the nanocrystals is also uniform. Moreover, the position of the long-wavelength band at 780 nm is thought to result from the non-spherical shape of silver particles.[18,19] Indeed, a correlation was observed between this band and the presence of such objects. When comparing spectrum E in Fig. 1 to that presented in Fig. 7, it is evident that spirooxazine molecules in the presence of PVP not only reduce the silver ions but also have a strong influence on the size and structure of the silver particles formed. Similarly, PVP is a good protective agent and may also contribute to the reduction of the Ag^+ ions in the presence of alcohol.[20] One of the mechanisms responsible for in-plane growth is direct reduction of silver ions on the surface of primary colloidal particles by accumulated electrons, which were previously transferred from the adsorbed and partially oxidized (one electron) spirooxazine species.[21]

Since the reduction of silver ions proceeds from the open Mc form, UV irradiation was applied for photoinduced preparation of the Ag sol. Silver colloids formed after 1 h exposure to 350 nm light are in fact similar to those observed in the thermal reaction, although the growth process is much faster. Two absorption maxima, corresponding to small spheres and larger silver objects, such as large lumps of coalesced particles or regular nanocrystals, are again observed. Upon increasing the irradiation time, the 420 nm absorption peak fades away while the 790 nm absorption band shifts towards the blue region with a progressive increase in its intensity. A blue colour is observed for the final colloid. The change in size distribution towards bigger sizes at the expense of smaller clusters upon UV irradiation is clearly supported by light scattering (photo correlation spectroscopy, PCS) experiments (Fig. 8). The changes in the absorption peak located at 790 nm are possibly due to an increase in the number of strong particle–particle interactions and/or increasing uniformity of the silver nanocrystallites formed. The absence of small particles or condensed objects is further evidenced by TEM. The photoinduced corrosion of the small particles is probably related to the absorption and excitation of the dye molecules at irradiation wavelengths, as silver particles do not absorb light at these wavelengths. The low intensity UV light used in the experiment excludes the possibility of direct excitation of silver particles.[22] The absorption spectra reported in Fig. 8 and the absence of fluorescence from the "blue" colloidal sample indicate that the reduced form of spirooxazine is present during the growth and morphological changes of the silver particles.

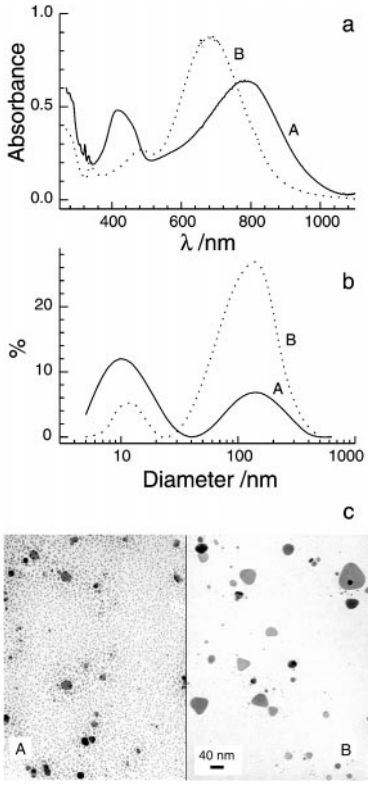

Fig. 8 Formation and evolution of colloidal silver solution upon UV irradiation. (a) Extinction spectra of the solution after 1 h (A) and 3 h (B) of UV illumination. (b) PCS diagrams of the samples corresponding to the UV-vis spectra. (c) TEM micrographs of the same samples.

Conclusions

Photochromic spiro compounds readily undergo oxidation when a carbon atom is replaced by nitrogen to form a naphthopyran heterocycle. The oxidation of two representatives of the spirooxazines was studied in the presence of Ag^+ ions. The similarity of the rearranged products, involving the oxazole ring, suggests a general mechanism for the thermal degradation in the spirooxazine family. A two-step electron transfer between the zwitterionic Mc form of a parent spirooxazine and the electron acceptor Ag^+ is proposed. There are two sites in Mc from which direct electron transfer takes place: the first one occurs at the O4′ oxygen atom, the second one either at the O4′ or C2′ carbon. Accordingly, the fatigue resistance of spirooxazines could be greatly improved by replacing the proton on the C2′ carbon by a substituent having neutral electronic or weak electron-withdrawing properties and simultaneously small steric hindrance.

The unusual growth and size modification of silver nanoparticles in PVP was attributed to chemisorption of partially oxidized merocyanine (one electron). The binding implies that silver clusters may be intermediates in the reduction of Ag^+ ions by accepting the second electron from the dye. These results could be interesting with respect to the role of silver colloids in surface-enhanced phenomena, non-linear optics and catalysis.[17] Another context of this work is photographic science and the problem of spectral sensitising (*e.g.*, by cyanine dyes[23]) of photographic material or colour development by organic dyes.[24] In both cases an electron is transferred from the dye molecule to the silver halide particles and a latent image centred on the surface of the grain is produced.[25] The high sensitivity of the spirooxazines towards thermal and photoreduction reactions could be used for chemical sensing of silver ions using fluorescence, for example.

Experimental

Materials

Photochromes 1,3-dihydro-1,3,3-trimethylspiro(2*H*-indole-2,3′-[3*H*]naphth[2,1-*b*]-[1,4]oxazine) (**1**), 1,3-dihydro-1,3,3-trimethylspiro(2*H*-indole-2,3′-[3*H*]phenanthr[9,10-*b*]-[1,4]oxazine) (**2**) and poly(*N*-vinylpyrrolidone) (PVP) with a weight average number of 4×10^4 were purchased from Aldrich Chemical Co. and used as received. Silver nitrate ($AgNO_3$, analytical reagent) was obtained from Billault (France). All solvents (methanol, acetonitrile) were dried over appropriate drying agents and distilled immediately prior to use under argon. Absolute ethanol (Aldrich) was used as received. All reactions were performed under an atmosphere of argon using standard Schlenk line techniques. All UV irradiations of spirooxazine solutions were carried out with a fluorescence photochemical reactor lamp (8 W) with the maximum intensity at 350 nm.

Spectroscopic measurements

UV-visible and infrared absorption spectra were obtained with an HP diode array 8452A spectrophotometer and with either an ITI Mattson Infinity FT system or a Perkin–Elmer 2000. Room-temperature excitation and emission spectra were acquired with a Perkin–Elmer LS50 luminescence spectrometer. Time resolved fluorescence measurements were performed with a system consisting of a nitrogen laser (300 ps, energy 78 μJ), a monochromator, a multiplier (2 ns response time), an oscilloscope and computer for data storage and analysis. The ^1H and ^{13}C NMR spectra were recorded at 305 K on a Bruker AMX400 spectrometer operating at 400.13 MHz for ^1H and at 100.61 MHz for ^{13}C. All chemical shifts for ^1H and ^{13}C were related to TMS using ^1H (residual) or ^{13}C chemical shifts of the solvent as a secondary standard. NMR studies were carried out either by one or two-dimensional NMR methods. The assignments of the ^1H resonances were made by 1D or 2D nuclear Overhauser exchange spectroscopy (NOESY) ($t_n = 600$ ms) and 1D total correlation spectroscopy (TOCSY) ($t_m = 60$ ms), whereas 2D heteronuclear correlation techniques (HMQC, HMBC) were used for the complete ^{13}C chemical shift assignments.

Crystallographic structural determination

The single-crystal X-ray diffraction data were collected at 180 K on a Stoe imaging plate diffraction system (IPDS) diffractometer with an Mo-Kα irradiation source ($\lambda = 0.71073$ Å, $\mu = 5.69$ cm^{-1}) and equipped with an Oxford Cryosystems Cryostream cooler device. Numerical corrections were applied that yielded chemically reasonable and computationally stable results of refinement. The structures were solved by direct methods using SIR92, and refined by least-squares procedures on F^2 with the SHELX97 program. All non-hydrogen atoms were refined with anisotropic displacement coefficients, while H atom positions were calculated on geometrical grounds as idealized contributions.

CCDC reference numbers 171832–171835. See http://www.rsc.org/suppdata/nj/b1/b105446p/ for crystallographic data in CIF or other electronic format.

Preparation and characterization of colloidal silver

The photochrome (2×10^{-5} mol) and PVP (0.4 g) were dissolved in 10 mL of ethanol. The solution was placed in a Pyrex flask with magnetic stirrer and deaerated under vacuum. In order to prepare colloidal silver, 10^{-4} mol of $AgNO_3$ was added under argon. The solution was irradiated by 350 nm UV light at ambient temperature (20 °C). Optical spectra were recorded in a quartz cell of 1 mm path length. Electron

micrographs (TEM) were taken with a JEOL transmission electron microscope model 200CX. The particle size distribution was obtained from a sample placed on a copper grid coated with amorphous carbon or from a Malvern Instruments Zetasizer 3000HSA, which allows sizing measurement using photon correlation spectroscopy (PCS).

Reactions of 1 and 2 with $AgNO_3$

The appropriate photochrome (2×10^{-5} mol) was dissolved in deaerated alcohol (5 mL) and 4×10^{-5} mol of silver nitrate was added. After several minutes the solution turned pale brown (**1**) or pale orange (**2**) and then the colouration become deeper with time. The reaction mixture was filtered and left standing at 4 °C overnight. Pale beige crystals precipitated from solution. From the remaining mixture, the solvent was evaporated and the samples were again dissolved in deuterated solvents.

Spectroscopic data

3. ^{1}H NMR (CD_3OD): δ 8.67 (d, $^3J_{HH} = 8.2$ Hz; 1H, C10′-H), 8.30 (d, $^3J_{HH} = 9.1$ Hz; 1H, C6′-H), 8.16 (d, $^3J_{HH} = 8.1$ Hz; 1H, C7′-H), 8.10 (dd, $^3J_{HH} = 6.8$ Hz; $^4J_{HH} = 2.0$ Hz; 1H, C7-H), 8.04 (d, $^3J_{HH} = 9.1$ Hz; 1H, C5′-H), 7.90 (d, $^3J_{HH} = 7.1$ Hz; 1H, C4-H), 7.87 (dd, $^3J_{HH} = 8.2$ Hz, $^3J_{HH} = 7.0$ Hz; 1H, C9′-H), 7.79 (dd, $^3J_{HH} = 7.4$ Hz, $^3J_{HH} = 7.1$ Hz; 1H, C5-H), 7.77 (dd, $^3J_{HH} = 7.4$ Hz, $^3J_{HH} = 6.8$ Hz; 1H, C6-H), 7.76 (dd, $^3J_{HH} = 8.1$ Hz, $^3J_{HH} = 7.0$ Hz; 1H, C8′-H), 4.82 (s; 3H, N^+–CH_3), 2.07 (s; 6H, *gem*-CH_3). ^{13}C NMR (CD_3OD): δ 170.21 (C2), 55.40 (C3), 123.38 (C4), 143.92 (C4a), 131.59 (C5), 130.75 (C6), 116.51 (C7), 142.96 (C7a), 37.81 (C8), 24.45 (C9, C10), 151.28 (C2′), 150.41 (C4′a), 111.15 (C5′), 134.22 (C6′), 132.49 (C6′a), 129.67 (C7′), 127.85 (C8′), 129.55 (C9′), 122.33 (C10′), 126.65 (C10′a), 138.42 (C11′). IR (solid phase): 1333 cm^{-1} (NO_3).

3a. ^{1}H NMR (CD_3CN): δ 8.44 (C10′-H), 7.79 (C6′-H), 7.93 (C7′-H), 6.64 (C7-H), 8.70 (C5′-H), 7.09 (C4-H), 7.71 (C9′-H), 6.79 (C5-H), 7.17 (C6-H), 7.56 (C8′-H), 3.43 (OH), 2.87 (s; 3H, N–CH_3), 1.51 (C10-CH_3), 0.88 (C11-CH_3).

1,3-Dihydro-1,3,3-trimethylspiro-2′-methoxy-(2*H*-indole-2,3′-[3*H*]naphth[2,1-*b*]-[1,4]oxazine), 4. ^{1}H NMR ($CDCl_3$): δ 8.52 (d, $^3J_{HH} = 8.1$ Hz; 1H, C10′-H), 7.80 (d, $^3J_{HH} = 8.1$ Hz; 1H, C7′-H), 7.61 (d, $^3J_{HH} = 8.8$ Hz; 1H, C6′-H), 7.55 (ddd, $^3J_{HH} = 8.1$ Hz, $^3J_{HH} = 6.8$ Hz, $^4J_{HH} = 1.3$ Hz; 1H, C9′-H), 7.41 (ddd, $^3J_{HH} = 8.1$ Hz, $^3J_{HH} = 6.8$ Hz, $^5J_{HH} = 1.3$ Hz; 1H, C8′-H), 7.20 (ddd, $^3J_{HH} = 8.0$ Hz, $^3J_{HH} = 7.8$ Hz, $^5J_{HH} = 1.1$ Hz; 1H, C6-H), 7.14 (d, $^3J_{HH} = 8.8$ Hz; 1H, C5′-H), 7.00 (dd, $^3J_{HH} = 7.4$ Hz, $^4J_{HH} = 1.1$ Hz; 1H, C4-H), 6.82 (ddd, $^3J_{HH} = 7.8$ Hz, $^3J_{HH} = 7.4$ Hz, $^5J_{HH} = 0.9$ Hz; 1H, C5-H), 8.52 (d, $^3J_{HH} = 8.0$ Hz; 1H, C7-H), 4.10 (s; 3H, O–CH_3), 2.96 (s; 3H, N–CH_3), 1.24 (s; 3H, C9-H_3), 1.21 (s; 3H, C10-H_3). ^{13}C NMR ($CDCl_3$): δ 102.77 5 (C2), 51.91 (C3), 136.67 (C4a), 121.74 (C4), 119.11 (C5), 128.26 (C6), 106.31 (C7), 148.48 (C7a), 29.92 (C8), 25.78 (C9), 23.59 (C10), 157.05 (C2′), 143.39 (C4′a), 116.99 (C5′), 126.55 (C6′), 130.05 (C6′a), 128.02 (C7′), 124.34 (C8′), 126.46 (C9′), 122.28 (C10′), 130.11 (C10′a), 124.41 (C11′), 54.17 (C12′). IR (solid phase): 1639, 1608, 1489, 1462, 1380, 1324, 1298, 1271, 1253, 1233, 1208, 1099, 1087, 1029, 1002, 915, 811, 745 cm^{-1}. Anal. calc. for $C_{23}H_{22}N_2O_2$: C, 77.00; H, 6.14; N, 7.81; found: C, 77.05; H, 6.18; N, 7.79%.

5. ^{1}H NMR (CD_3CN): δ 7.91 (C4-H), 7.82 (C5-H), 7.80 (C6-H), 8.00 (C7-H), 4.76 (N^+–CH_3), 2.09 (*gem*-CH_3), 8.74 (C5′-H), 7.94 (C6′-H), 7.93 (C7′-H), 8.92 (C8′-H), 8.96 (C9′-H), 8.00 (C10′-H), 7.94 (C11′-H), 8.61 (C12′-H). ^{13}C NMR (CD_3CN): δ 169.72 (C2), 55.65 (C3), 123.69 (C4), 143.79 (C4a), 131.82 (C5), 130.32 (C6), 116.76 (C7), 142.97 (C7a), 38.43 (C8), 24.60 (C9, C10), 150.82 (C2′), 137.60 (C4′a), 125.09 (C5′a), 123.54 (C5′), 129.18 (C6′), 129.34 (C7′), 127.85 (C8′), 129.26 (C8′a), 132.87 (C9′a), 124.91 (C9′), 130.95 (C10′), 129.07 (C11′), 123.54 (C12′), 119.34 (C12′a), 149.42 (C13′). IR (solid phase): 1330 cm^{-1} (NO_3).

5a. ^{1}H NMR (DMSO-d_6): δ 7.09 (C4-H), 6.75 (C5-H), 7.15 (C6-H), 6.66 (C7-H), 2.96 (N-C8-H3), 1.58 (C9-H3), 0.83 (C10-H3), 8.73 (C4′-H), 7.94 (C5′-H), 7.93 (C6′-H), 8.92 (C7′-H), 8.96 (C8′-H), 8.00 (C9′-H), 7.94 (C10′-H), 8.61 (C11′-H), 3.49 (C2-OH). ^{13}C NMR (CD_2Cl_2): δ 99.02 (C2), 50.23 (C3), 122.6 (C4), 136.90 (C4a), 119.18 (C5), 128.48 (C6), 107.83 (C7), 149.43 (C7a), 30.49 (C8), 21.15 (C9), 27.41 (C10), 164.84 (C2′), 134.43 (C4′a), 126.44 (C5′a), 123.17 (C5′), 128.79 (C6′), 127.45 (C7′), 125.23 (C8′), 129.26 (C8′a), 129.57 (C9′a), 125.04 (C9′), 128.00 (C10′), 128.90 (C11′), 121.41 (C12′), 119.18 (C12′a), 145.06 (C13′).

1,3-Dihydro-1,3,3-trimethylspiro(2*H*-indole-2,3′-[3*H*]phenanthr[9,10-*b*]-[1,4]oxazine), 6. ^{1}H NMR ($CDCl_3$): δ 8.66 (dd, $^3J_{HH} \approx 6.3$ Hz, 1H, C8′-H), 8.64 (dd, $^3J_{HH} \approx 8.1$ Hz, 1H, C9′-H), 8.66 (dd, $^3J_{HH} \approx 8.0$ Hz, 1H, C12′-H), 8.17 (ddd, $^3J_{HH} = 7.9$ Hz, $J_{HH} = 0.9$ Hz; 1H, C5′-H), 7.69 (ddd, $^3J_{HH} = 8.0$ Hz, $^3J_{HH} = 7.0$ Hz, $^5J_{HH} = 1.2$ Hz; 1H, C11′-H), 7.62 (ddd, $^3J_{HH} = 7.0$ Hz, $^3J_{HH} = 7.0$ Hz, $^5J_{HH} = 1.5$ Hz; 1H, C7′-H), 7.60 (ddd, $^3J_{HH} = 8.1$ Hz, $^3J_{HH} = 7.0$ Hz, $^5J_{HH} = 1.0$ Hz; 1H, C10′-H), 7.56 (ddd, $^3J_{HH} = 7.0$ Hz, $^3J_{HH} = 7.0$ Hz, $^5J_{HH} = 1.2$ Hz; 1H, C6′-H), 7.23 (ddd, $^3J_{HH} = 7.7$ Hz, $^3J_{HH} = 7.7$ Hz, $^5J_{HH} = 1.2$ Hz; 1H, C6-H), 6.99 (dd, $^3J_{HH} = 7.2$ Hz, $^3J_{HH} = 0.8$ Hz; 1H, C4-H), 6.84 (ddd, $^3J_{HH} = 7.5$ Hz, $^3J_{HH} = 7.5$ Hz, $^5J_{HH} = 0.9$ Hz; 1H, C5-H), 6.63 (d, $^3J_{HH} = 7.7$ Hz, 1H, C7-H), 4.12 (s; 3H, O–CH_3), 3.02 (s; 3H, N–CH3), 1.28 (s; 3H, C9-H3), 1.26 (s; 3H, C10-H3). ^{13}C NMR ($CDCl_3$): δ 103.08 (C2), 51.47 (C3), 135.81 (C4a), 121.79 (C4), 119.12 (C5), 128.26 (C6), 106.48 (C7), 30.84 (C8), 25.87 (C9), 23.89 (C10), 157.24 (C2′), 138.21 (C4′a), 125.03 (C5′a), 122.44 (C5′), 127.03 (C6′), 126.62 (C7′), 123.01 (C8′), 129.89 (C8′a), 127.27 (C9′a), 122.89 (C9′), 125.10 (C10′), 127.22 (C11′), 122.86 (C12′), 129.90 (C12′a), 121.12 (C13′), 54.30 (C14′). IR (solid phase): 1641, 1617, 1607, 1491, 1450, 1363, 1324, 1289, 1264, 1201, 1109, 1098, 1025, 910, 758, 737, 726 cm^{-1}. Anal. calc. for $C_{27}H_{24}N_2O_2$: C, 79.32; H, 5.87; N, 6.85; found: C, 79.38; H, 5.90; N, 6.81%

1,3-Dihydro-5-nitro-1,3,3-trimethylspiro-2′-ethoxy-(2*H*-indole-2,3′-[3*H*]naphth[2,1-*b*]-[1,4]oxazine), 7. ^{1}H NMR ($CDCl_3$): δ 8.47 (dd, $^3J_{HH} = 8.2$ Hz; 1H, C10′-H), 8.21 (dd, $^3J_{HH} = 8.7$ Hz, $^4J_{HH} = 2.6$ Hz; 1H, C6-H), 7.85 (d, $^4J_{HH} = 2.6$ Hz; 1H, C4-H), 7.79 (d, $^3J_{HH} = 8.3$ Hz; 1H, C7′-H), 7.62 (d, $^3J_{HH} = 8.7$ Hz; 1H, C6′-H), 7.55 (ddd, $^3J_{HH} = 8.2$ Hz, $^3J_{HH} = 6.9$ Hz, $^4J_{HH} = 1.3$ Hz; 1H, C9′-H), 7.43 (ddd, $^3J_{HH} = 8.3$ Hz, $^3J_{HH} = 6.9$ Hz, $^4J_{HH} = 1.2$ Hz; 1H, C8′-H), 7.14 (d, $^3J_{HH} = 8.7$ Hz; 1H, C5′-H), 6.52 (d, $^3J_{HH} = 8.7$ Hz, 1H, C7-H), 4.58 (s; 2H, C12′-H2–), 3.05 (s; 3H, N–CH_3), 1.41 (dd; $^3J_{HH} = 7.1$ Hz; 3H, C13′-H3), 1.31 (s; 3H, C9-H3), 1.27 (s; 3H, C10-H3). IR (solid phase): 1739, 1642, 609, 1506, 1472, 1436, 1379, 1367, 1322, 1269, 1250, 1232, 1092, 1084, 811, 729, 719 cm^{-1}. Anal. calc. for $C_{24}H_{23}N_3O_4$: C, 68.99; H, 5.51; N, 10.06; found: C, 69.05; H, 5.60; N, 9.95%

Acknowledgements

This work was completed with the support of the European Associated Laboratory financed by CNRS (France) and the Polish Committee for Scientific Research (KBN 7 T08E 018 17 project). We thank Dr P. Balczewski for valuable discussions and V. Colliere for technical assistance with the TEM experiments.

References

1 R. C. Bertelson, in *Organic Photochromic and Thermochromic Compounds*, ed. J. C. Crano and R. J. Guglielmetti, Kluwer Academic/Plenum Publishers, New York, 1999, vol. 1, ch. 1.
2 V. Malatesta, in *Organic Photochromic and Thermochromic Compounds*, ed. J. C. Crano and R. J. Guglielmetti, Kluwer Academic/Plenum Publishers, New York, 1999, vol. 2, ch. 2.
3 V. Malatesta, M. Milosa, R. Millini, L. Lanzini, P. Bortolus and S. Monti, *Mol. Cryst. Liq. Cryst.*, 1994, **246**, 303.
4 V. Malatesta, R. Millini and L. Montanari, *J. Am. Chem. Soc.*, 1995, **117**, 6258.
5 I. Willner, *Acc. Chem. Res.*, 1997, **30**, 347.
6 F. Wilkinson, D. R. Worrall, J. Hobley, L. Jansen, S. L. Williams, A. J. Langley and P. Matousek, *J. Chem. Soc., Faraday Trans.*, 1996, **92**, 1331.
7 S. Schneider, F. Baumann, U. Kluter and M. Melzig, *Ber. Bunsen-Ges. Phys. Chem.*, 1987, **91**, 1225.
8 J. Aubard, in *Organic Photochromic and Thermochromic Compounds*, ed. J. C. Crano and R. J. Guglielmetti, Kluwer Academic/Plenum Publishers, New York, 1999, vol. 2, ch. 8.
9 J. Aubard, K. Karlsson, R. Dubest, G. Levi, B. Luccioni-Houze, C. Salemi-Delvaux and R. Guglielmetti, *Mol. Cryst. Liq. Cryst.*, 1997, **298**, 37.
10 K. Kimura, T. Yamashita, M. Kaneshige and M. Yokoyama, *J. Chem. Soc., Chem. Commun.*, 1992, 969.
11 M. J. Preigh, F.-T. Lin, K. Z. Ismail and S. G. Weber, *J. Chem. Soc., Chem. Commun.*, 1995, 2091.
12 P. Rys, R. Weber and Q. Wu, *Can. J. Chem.*, 1993, **71**, 1828.
13 S. Aldoshin, in *Organic Photochromic and Thermochromic Compounds*, ed. J. C. Crano and R. J. Guglielmetti, Kluwer Academic/Plenum Publishers, New York, 1999, vol. 2, ch. 7.
14 W. Clegg, N. C. Norman, T. Flood, L. Sallans, W. S. Kwak, P. L. Kwiatkowski and J. G. Lasch, *Acta Crystallogr., Sect. C*, 1991, **47**, 817.
15 S. Maeda, in *Organic Photochromic and Thermochromic Compounds*, ed. J. C. Crano and R. J. Guglielmetti, Kluwer Academic/Plenum Publishers, New York, 1999, vol. 1, ch. 2.
16 C. F. Bohren and D. R. Huffman, *Absorption and Scattering of Light by Small Particles*, John Wiley, New York, 1983 .
17 U. Kreibig and M. Vollmer, *Optical Properties of Metal Clusters*, Springer–Verlag, Berlin and Heidelberg, Germany, 1995 .
18 J. Belloni, M. Mostafavi, H. Remita, J. L. Marignier and M.-O. Delcourt, *New J. Chem.*, 1998, **22**, 1239.
19 D. C. Skillman and C. R. Berry, *J. Chem. Phys.*, 1968, **48**, 3297.
20 H. H. Huang, X. P. Ni, G. L. Loy, C. H. Chew, K. L. Tan, F. C. Loh, J. F. Deng and G. Q. Xu, *Langmuir*, 1996, **12**, 909.
21 A. Henglein and M. Giersig, *J. Phys. Chem. B*, 1999, **103**, 9533.
22 N. Chandrasekharan, P. V. Kamat, J. Hu and G. Jones II, *J. Phys. Chem. B*, 2000, **104**, 11 103.
23 L. Jeunieau, V. Alin and J. B. Nagy, *Langmuir*, 2000, **16**, 597.
24 J.-L. Marignier, *La Photochimie*, 1993, 85.
25 J. Belloni, in *Homogeneous Photocatalysis*, ed. M. Chanon, John Wiley & Sons Ltd., New York, 1997.